AD_____
(Leave blank)

Award Number:
W81XWH-08-1-0467

TITLE:
Characterization of the Truncated Androgen Receptor Generated by Calpain-Dependent Proteolysis in Prostate Cancer

PRINCIPAL INVESTIGATOR:
Honglin Chen Ph.D.

CONTRACTING ORGANIZATION:
University of California Davis
Davis, CA 95616

REPORT DATE:
August 2009

TYPE OF REPORT:
Annual Summary

PREPARED FOR: U.S. Army Medical Research and Materiel Command
Fort Detrick, Maryland 21702-5012

DISTRIBUTION STATEMENT: (Check one)

X Approved for public release; distribution unlimited

Distribution limited to U.S. Government agencies only; report contains proprietary information

The views, opinions and/or findings contained in this report are those of the author(s) and should not be construed as an official Department of the Army position, policy or decision unless so designated by other documentation.

# REPORT DOCUMENTATION PAGE

*Form Approved*
*OMB No. 0704-0188*

Public reporting burden for this collection of information is estimated to average 1 hour per response, including the time for reviewing instructions, searching existing data sources, gathering and maintaining the data needed, and completing and reviewing this collection of information. Send comments regarding this burden estimate or any other aspect of this collection of information, including suggestions for reducing this burden to Department of Defense, Washington Headquarters Services, Directorate for Information Operations and Reports (0704-0188), 1215 Jefferson Davis Highway, Suite 1204, Arlington, VA 22202-4302. Respondents should be aware that notwithstanding any other provision of law, no person shall be subject to any penalty for failing to comply with a collection of information if it does not display a currently valid OMB control number. **PLEASE DO NOT RETURN YOUR FORM TO THE ABOVE ADDRESS.**

| 1. REPORT DATE | 2. REPORT TYPE | 3. DATES COVERED |
|---|---|---|
| 8/31/09 | Annual Summary | 1 AUG 2008 - 31 JUL 2009 |

**4. TITLE AND SUBTITLE**

Characterization of the Truncated Androgen Receptor Generated by Calpain-Dependent Proteolysis in Prostate Cancer

**5a. CONTRACT NUMBER**
W81XWH-08-1-0467

**5b. GRANT NUMBER**

**5c. PROGRAM ELEMENT NUMBER**

**6. AUTHOR(S)**

Honglin Chen Ph.D.

Email: hlchen@ucdavis.edu

**5d. PROJECT NUMBER**

**5e. TASK NUMBER**

**5f. WORK UNIT NUMBER**

**7. PERFORMING ORGANIZATION NAME(S) AND ADDRESS(ES)**

University of California Davis
Davis, CA 95616

**8. PERFORMING ORGANIZATION REPORT NUMBER**

**9. SPONSORING / MONITORING AGENCY NAME(S) AND ADDRESS(ES)**

U.S. Army Medical Research and Materiel Command
Fort Detrick, Maryland 21702-5012

**10. SPONSOR/MONITOR'S ACRONYM(S)**

**11. SPONSOR/MONITOR'S REPORT NUMBER(S)**

**12. DISTRIBUTION / AVAILABILITY STATEMENT**

Approved for Public Release; Distribution Unlimited

**13. SUPPLEMENTARY NOTES**

**14. ABSTRACT**

Androgen ablation therapy is effective in treating androgen-dependent prostate tumors; however, tumors that can proliferate in castrate levels of androgen eventually arise. We previously reported that in CWR22Rv1 (Rv1) cells, the protease calpain 2 can cleave the androgen receptor (AR) into a constitutively active ~80 KDa low molecular weight (LMW) form. In this study, we further dissect the mechanisms that produce the AR LMW forms using Rv1 cells and the related CWR22-R1 (R1) cells. The 39 a.a. insertional mutation in Rv1 cells sensitizes this AR (E3DM-AR) calpain 2 proteolysis. R1 cells encode the same AR molecule as the parental CWR22 xenograft. Using anti-calpain 2 siRNA and calpeptin, we find that calpain 2 plays a role in the generation of the LMW-AR in R1 cells. Furthermore, LMW-AR expression is regulated by the activation of calpain 2 by Extracellular Signal-Regulated Kinases 1/2 (ERK). Inhibition of ERK phosphorylation or siRNA-mediate decrease of ERK expression reduces LMW-AR levels in R1 cells. Conversely, activation of the MAPK pathway and increased ERK phosphorylation results in increased levels of LMW-AR. Finally, analyses of human tumor samples found that LMW-AR levels are higher in tumors that have an increased calpain/calpastatin ratio and/or increased levels of phospho-ERK (pERK), suggesting that a higher calpain/calpastatin ratio collaborates with activation of the MAP kinase pathway to promote the generation of the LMW-AR. Furthermore, cellular localization analysis of AR shows that the LMW-AR is the predominant form (~90%) present in the nucleus in Rv1 cells cultured in the absence of androgen, allowing us to study the chromosomal binding sites of LMW-AR using chromatin immunoprecipitation (ChIP) combined with DNA microarray analysis (ChIP-on-chip). Using a human promoter array, a total of 128 potential LMW-AR chromosomal binding sites are identified in the absence of androgen and they are also present in the presence of androgen. We find that the majority of the binding sites contain no AR-responsive elements (AREs) and are distant (>2kb) from the transcriptional start sites. Corresponding expression array studies identify that only a subset of genes in the vicinity of LMW-AR binding sites respond to the stimulation of dihydrotestosterone (DHT). Moreover, quantitative RT-PCR analysis shows that LMW-AR can transcriptoinally regulate certain genes in a different manner as full-length (FL) AR.

**15. SUBJECT TERMS**

low-molecular weight androgen receptor, full-length androgen receptor, calpain, ERK, calpastatin, Chip-on-Chip

| 16. SECURITY CLASSIFICATION OF: | | | 17. LIMITATION OF ABSTRACT | 18. NUMBER OF PAGES | 19a. NAME OF RESPONSIBLE PERSON |
|---|---|---|---|---|---|
| a. REPORT | b. ABSTRACT | c. THIS PAGE | | | USAMRMC |
| U | U | U | UU | 29 | 19b. TELEPHONE NUMBER *(include area code)* |

## Table of Contents

**Page**

## Introduction

Prostate cancers are a commonly diagnosed malignancy that is treated with hormonal therapy aimed at blocking signaling through the AR. Initially most prostate cancers present are androgen-dependent neoplasms, thus the clinical response is positive. Unfortunately, aggressive cancers that proliferate in castrate levels of androgens eventually develop. Analysis of clinical relapsed tumor revealed that over 90% express the AR [1-4]. The AR is central to the initiation and growth of prostate cancers and in their responses to therapy. The AR is a member of the steroid hormone superfamily of ligand-activated transcription factors that include the progesterone and glucocorticoid receptors [5, 6], and contains four functional domains: an N-terminal regulatory region, a DNA-binding domain (DBD), a hinge domain and a ligand binding domain (LBD) [7]. In the absence of ligand, the AR is retained in the cytoplasm. The binding of hormone to the LBD alters AR conformation promoting dimerization, phosphorylation, and translocation into the nucleus, allowing for the recruitment of proteins into the transcription initiation complex [6, 8, 9].

During tumor progression, tumors acquire the ability to proliferate in castrate levels of androgen. Alterations of AR have been postulated to account for the aberrant AR activation and acquisition of proliferative capabilities in reduced levels of androgen. Studies have shown that 25-30% of androgen independent tumors that arose following endocrine therapy have an amplification of the AR gene [10, 11]. AR mutations are more common in androgen independent cancers [12, 13]. In most cases, AR mutations broaden ligand specificity so that mutated AR can be activated more efficiently by various steroids [7]. The well studied androgen responsive cell lines LNCaP and MDA PCa have mutations in the LBD that broadens the ligand specificity, allowing for activation by estrogens, progesterone, glucocorticoids and adrenal androgens [14-16]. The CWR22 xenograft has a mutation in the LBD that enhances responsiveness to estradiol and progesterone [17]. Structure function analysis of the AR showed that deletion of the LBD generates a constitutively active molecule [18]. This *in vitro* analysis was validated by a report which described a point mutation at Q640 that resulted in a C-terminally truncated and constitutively active AR [19]. The latter studies imply that AR truncation may be a mechanism in the etiology of androgen independent tumors. Others and we previously reported that the calpain protease could cleave the AR molecule to LMW isoforms [20-22], including a ~80 KDa C-terminally truncated. We also reported that ~ 80KDa LMW-AR is present in some human prostate tumors [21]. Using the androgen-independent cell line model CWR22Rv1 expressing high level of the LMW-AR, we have shown that inhibition of calpain activity induces apoptosis in the cells cultured in the absence of androgen and statistically-significant inhibition of tumor growth in castrated CWR22rv1 xenografts. These studies implicate that the LMW-AR generated by calpain-dependent proteolysis of the AR may play an important role in conferring androgen-independence in a subset of prostate cancer [21].

ChIP-on-chip has recently emerged as the staple of studying genome-wide chromosomal binding sites of transcription factors and identifying their novel targets [23, 24]. Despite the well-characterized androgen response elements (AREs) in the promoter and enhancer of prostate-specific antigen (PSA), little is known about AR *cis*-regulatory sites across the human genome. Wang et al., [25] used a tiling DNA microarray combined with ChIP to map the AR binding regions on chromosome 21 and 22 in androgen-dependant LNCaP cells. In the 90 AR binding sites identified on the two chromosomes, they reported that the majority AR binding regions contain noncanonical AREs and are far (>10kb) from the transcriptional start sites of androgen-regulated genes. Another group performed ChIP-on-chip in LNCaP cells using a sampler DNA microarray called ENCODE chip which represents approximately 1% of the whole genome [26]. They found that most of the AR-interacting regions are located in non-

promoter proximal regions. Interestingly, similar results have been shown on the binding sites of estrogen receptor (ER), another ligand-dependant nuclear receptor [27]. These studies indicate the complexity of the *cis*-regulation by these nuclear receptor transcription factors.

Two cell lines, CWR22Rv1 (Rv1) and CWR22R1 (R1), that proliferate in castrate levels of androgens were isolated in two laboratories from CWR22 relapse tumors. CWR22, an androgen-dependent, serially transplantable xenograft model was derived from a primary human prostate cancer and recapitulates salient feature of prostate cancer progression in patients [28]. The AR in the CWR22 xenograft has a mutation (H847Y) in the LBD of the molecule [17]. Like parental CWR22 cells, Rv1 and R1 cells express the AR containing the point mutation, while Rv1 AR also contains a duplication of DBD encoding exon3, which results in an insertion of 39 additional amino acids [29]. A previous study found that the R1 cell line also expresses a ~80KDa LMW AR isoform, but to a less extent than Rv1 cells [30]. The mechanism resulting in the expression of the LMW-AR in R1 cells has not been reported.

**Body**

There are some deviations from the original Statement of Work (SOW). After the submission of the application, we were able to obtain an additional line CWR22R1 (R1) which also express the LMW-AR. Therefore, we were interested in investigating whether the mechanism leading to the generation of LMW-AR in R1 cells are different from that of Rv1 cells. This part of study was not in the original SOW. Also, in the original SOW, we planned to use these two artificial sublines of CWR22Rv1 (CWR22rv1-fl-AR expressing exogenous fl-AR only and CWR22rv1-tr- AR expressing exogenous tr-AR only) to study the DNA binding pattern and gene expression profiles of LMW-AR and fl-AR. During the research, we found that the LMW-AR is the predominant form (~90%) present in the nucleus in Rv1 cells cultured in the absence of androgen, which allows the study of the potential LMW-AR specific chromosomal binding sites. Using this native cell model is a better approach than artificial sublines for this study purpose. In summary, we have expanded the tasks listed in SOW. So far, the task 1 and 2 listed in SOW has almost be completed. Task 3 and 4 haven't been conducted. Following is the results completed in this time period.

***Characteristics of the Rv1 and R1 cell lines.***

Two castrate resistant cells lines, R1 and Rv1, were derived from two independent CWR22 relapsed tumors. The cellular phenotypes of the Rv1 and R1 cells are similar. In the presence of androgen the cells tend to grow in clusters, while in the absence of androgens they tend to be more scattered and less adhesive (Figure 1A). The AR in both lines has the same LBD mutation as the CWR22 xenograft [17]. As previously reported, R1 and Rv1 cells express the LMW AR forms [29, 31] (Figure 1B). Western immunoblot analysis indicated that R1 cells expressed higher levels of AR than Rv1 cells, but the ratio of the LMW to full length (FL)-AR was higher in Rv1 cells. The size of the FL-AR in the R1 cells is smaller than the FL-AR in the Rv1 cells, since R1 cells do not have the 39 amino acid duplication of exon 3. Closer inspection revealed that the ~80 KDa LMW forms could be resolved into several discrete bands (Figure 1B). The MTS proliferation assay confirmed that the R1 and Rv1 cell proliferation rates were only slightly slower in androgen-depleted media compared to the cell proliferation rates in the presence of androgen (Figure 1C). The proliferation assay conducted in the presence of 10 uM Casodex indicated that R1 and Rv1 cells were refractory to the inhibitory effects of this AR inhibitor (Figure 1D). While all three lines are responsive to androgen, only LNCaP cells are dependent on androgen to sustain growth.

***Generation of the LMW-AR involves calpain.***

We have reported previously that the inhibition of calpain activity by calpeptin reduces the levels of the expression of the LMW-AR in Rv1 cells [21]. Likewise, treatment of R1 cells proliferating in the presence or absence of androgen (Ad) with the calpeptin reduced the level of LMW-AR in R1 cells (Figure 2A). We previously showed that proteolysis of the calpain substrate focal adhesion kinase (FAK) is a good indicator of calpain activity [32]. Calpeptin treatment of R1 cells reduced the levels of LMW-FAK (Figure 2A). To further analyze the role of calpain in the generation of LMW-AR, calpain 2 expression was analyzed in several prostate tumor derived, as well as immortalized, prostate cell lines. R1 cell expressed much higher levels of calpain 2 than Rv1 and LNCaP cells (Figure 2B). Interestingly, the two AR negative and highly metastatic cells lines PC3 and DU145 expressed the highest levels of calpain 2. Given that calpain activity is regulated by its endogenous inhibitor calpastatin, we analyzed calpastatin levels as well, and found that expression was comparable in all the cell lines (Figure 2B). R1 cells had higher amounts of proteolyzed FAK, indicating greater calpain activity (Figure 2C). The

extent of FAK cleavage was greater in the absence of androgen, suggesting that calpain activity may be higher under androgen-depleted conditions. To further confirm the involvement of calpain 2 in the generation of the LMW-AR forms in R1 cells, we used anti-calpain 2 siRNA to reduce the calpain 2 expression. A previous study reported that calpain 2 has a very long half life of 5 days [33]. A 6-day treatment resulted in an ~60% reduction of calpain 2 protein level in R1 cells (Figure 2D) and reduced levels of the LMW-AR forms (Figure 2D). This treatment also reduced FAK proteolysis indicating that calpain 2 activity was reduced. This analysis indicates that calpain 2 plays a role in the generation of the LMW-AR in R1 cells.

R1 cell proliferation is not androgen dependent, however, R1 cells are androgen responsive since the expression of certain genes is androgen regulated. We found that the expression of claudin 4 (CLDN4) is highly repressed by the addition of androgen (Figure 2E). If calpeptin treatment reduces the levels of LMW-AR, then in the absence of androgen the expression of androgen repressed genes may be further activated. Calpeptin treatment of R1 cells further increased the expression of CLDN4, thus arguing the LMW-AR has a role in transcription of certain genes.

***The exon3 duplication sensitizes Rv1 AR to calpain proteolysis***

Rv1 cells express higher levels of the LMW-AR but have low expression of calpain 2 protein and calpain activity (Figure 2). We hypothesize that the exon 3 duplication sensitizes the E3DM-AR to calpain cleavage. The AR-null PC3 cells expressing high levels of calpain 2 were transfected with cDNAs plasmids encoding either the wildtype or E3DM-AR. As expected, the E3DM-AR was slightly larger than the wildtype receptor (Figure 3A). Additionally, the LMW forms expressed in cells transfected with the E3DM-AR were larger than the LMW forms expressed in cells transfected with the wildtype AR cDNA. To test the hypothesis that the E3DM-AR is more sensitive to calpain-dependent proteolysis, extracts prepared from the transfected cells were treated with $CaCl_2$ to activate the endogenous calpain activity. As shown in Figure 3B, the AR was progressively cleaved into the smaller forms by the addition of $CaCl_2$. The inclusion of calpeptin retarded proteolysis, indicating that proteolysis was calpain dependent (figure 3B). While the ~80 KDa forms were present initially and throughout the time course, as proteolysis progressed, the LMW-AR was further proteolyzed to smaller peptides. In vivo, the ~ 80 KDa LMW-AR forms that are generated by proteolysis can translocate into the nucleus, where they would be less susceptible to further proteolysis. In vitro, as was previously observed [20] activated calpain proteolyzes the AR to still smaller forms. The mutant E3DM-AR was cleaved more rapidly than the wildtype FL-AR, resulting in the disappearance of the FL-AR (compare lanes 4 and 9).

***The expression of the LMW-AR is regulated by the ERK kinase***

Calpain activity is tightly regulated by various mechanisms, including phosphorylation. Previous studies have shown that ERK can phosphorylate calpain 2 to stimulate protease activity [34]. ERK expression was analyzed in immortalized (RWPE-1, PZ-HPV-7 and pRNS-1-1) and tumor derived (PC3, LNCaP, Rv1, R1 and DU145) cell lines. All of the tumor derived cells lines had higher levels of ERK in comparison to the immortalized cell lines (Figure 4A). A comparison of R1 and Rv1 cells proliferating in the absence and presence of androgen showed that R1 cells had higher levels of the active form of the protein (pERK) under both conditions (Figure 4B).

ERK is phosphorylated and activated by MEK, a dual threonine and tyrosine kinase [34]. Treatment of R1 cells with the MEK inhibitor U0126 for 24 or 48 hours reduced ERK phosphorylation (Figure 4C). An analysis of the AR in the same extracts (Figure 4C) indicated

that inhibition of ERK activity reduced the levels of LMW-AR. Similar results were found in Rv1 cells(data not shown). To confirm that LMW-AR expression is dependent on ERK, cells were treated with control siRNA and ERK siRNA. Inhibition of ERK expression resulted in decreased levels of LMW-AR (Figure 4D). This analysis established that ERK activation has a role in the etiology of the LMW-AR forms.

Since the PKC activator phorbol ester 12-O-tetradecanoylphorbol-13-acetate (TPA) can result in ERK phosphorylation [35], Rv1 and R1 cells were treated with TPA in the absence of androgen for 1 or 2 hours to stimulate ERK activity. This treatment promoted an increase in levels of the LMW-AR indicating that activation of this pathway resulted in enhanced AR proteolysis (Figure 5A). TPA treatment of Rv1 cells also resulted in decreased levels of the FL-AR; after a 2 hour TPA treatment the FL-AR was barely discernable, arguing that in vivo, as in vitro, the Rv1 AR is more sensitive to proteolysis.

To test our hypothesis that an increase in calpain 2 and ERK activity collaborate in promoting LMW-AR expression we examined the calpain 2, calpastatin and pERK levels in 6 of 13 tumor samples previously analyzed for the expression of the LMW-AR. Three of the thirteen samples that had the highest levels LMW-AR (01, 31 and 94) and three that had low levels of LMW -AR (21, 25, and 28) were used in the analysis (Figure 5B). The expression of LMW-AR was defined as percent of total. Interestingly the levels of the endogenous calpain inhibitor calpastatin was variable and was higher in sample 21 and 25, which has lower levels of LMW-AR and lowest in Sample 01. Samples 01 and 31 had high levels of pERK (Figure 5C). The remaining samples had low pERK levels. Therefore, the three samples that had the highest LMW-AR had high levels of pERK or a high amount of calpain 2. Conversely, samples that had low LMW-AR levels had little pERK and had elevated calpastatin levels. This limited analysis suggests that in human tumors an increased ratio of calpain to calpastatin and increased ERK activity, in concert contribute to increased LMW- AR expression.

### *The LMW-AR binds to the chromosomal binding sites in the absence of androgen in Rv1 cells*

Previous studies reported that deletion of the LBD resulted in the translocation of the AR into the nucleus in the absence of androgen [19, 31]. Therefore we analyzed the cellular location of the LMW-AR in the nuclear and cytosolic fractions of Rv1 and R1 cells proliferating the presence and absence of androgen (Figure 6A). In R1 cells the predominant form of the AR in the nucleus in the presence of androgen is the FL-AR. In the absence of androgen the nuclear fraction contains substantially higher amount of the LMW-AR (~60%). In the cytosolic fraction the AR is almost exclusively full length. In Rv1 cells in the presence of androgen, the FL-AR and LMW-AR are present in the nucleus. The FL-AR is more abundant in the cytosol, whereas the LMW-AR is more abundant in the nucleus. Notably, in the absence of androgen the Rv1 nuclear fraction consists predominantly (~90%) of the LMW-AR. Therefore, we performed ChIP-on-chip analysis on Rv1 cells proliferating in androgen-depleted medium to investigate the potential LMW-AR chromosomal binding sites. The same analysis was conducted on Rv1 cells treated with 10nM DHT for 2hr and in R1 cells treated in the same manner. The study used the Human Promoter 1.0R Array (Affymetrix). This oligonucleotide (25-mer)-based, high-density tiling array covers 25,500 promoters with probe sets spanning approximately 10 kb of genomic content per gene (7.5 kb upstream and 2.45 kb downstream of the transcriptional start site) and at a resolution of 35 bp.

Analysis of the ChIP-on-chip data revealed 128 binding sites (FDR<=0.05) in Rv1 cells proliferating in androgen-depleted media (Table 1). Furthermore, the 128 sites were also present in the total of 2021 binding sites identified in Rv1 cells treated with 10nM DHT for 2hrs using the same criteria (i.e. FDR<=0.05) (Figure 6B, 6C). A closer examination of these 128

binding sites revealed that 20% of the sites showed exactly the same start and end position in the absence or presence of DHT. The remainder (80%) were within the range of ~35-1000bp upstream of the start position or downstream of the end position. Furthermore, the addition of androgen induced modest [1 going to 2] enrichment of AR binding to the sequence adjacent (within 50Kb) to 46 sites (46/128=36%), and high enrichment [3 or more] to the sequence adjacent to 14 sites (14/128=11%). Addition of androgen did not cause enrichment in the AR binding to the rest 68 sites (68/128=53%). Addition of androgen also resulted in the AR binding to sites that were not bound in the absence of androgen, indicating the requirement of the FL-AR for binding to specific sequences.

Next we compared AR binding in Rv1 and R1 cells cultured in androgen depleted media. Analysis of the ChIP-on-chip data obtained from R1 cells failed to reveal binding sites that were statistically significant (FDR<=0.05). Due to the low level of the AR (both FL- and LMW-AR) in the nucleus of R1 cells proliferating in androgen depleted media, the assay may not be sensitive enough to detect binding that reaches the threshold of statistical significance. Nevertheless, the examination of the best potential binding sites provided by Cisgenome showed that 15 binding sites overlapped with the binding sites identified Rv1 cells (Table 1 labeled with *). Furthermore, all these 15 sites were identified as statistical significant (FDR<=0.05) binding sites in R1 cells treated with DHT for 2hr (Figure 6B).

We analyzed the 128 binding sites to determine whether the LMW-AR binds to the established consensus AR response element (ARE). Wang et al., [25] reported that, in LNCaP cells treated with DHT, only 10% of the AR binding regions had a canonical class 1 ARE (AGAACAnnnTGTTCT) binding motif when two positions were allowed to vary from the palindromic consensus with 3 nucleotide spacing. They also found that 78% of the binding regions contained the AR binding half-site motif (AGAACA). In this study, using the similar motif mapping algorithm, we found 6% (8/128) of the LMW-AR binding sites contained the typical ARE (Table 2) and 48% contained the AR half-site motif. This indicates that, similar to the FL-AR in LNCaP cells, the LMW-AR predominantly binds to non-canonical AREs. Likewise, analysis of the 2021 binding sites identified in DHT treated Rv1 cells showed only 4% (86/2021) of the sites had the canonical ARE and 35% (700/2021) had the AR half-site motif (Figure 6D).

Further analysis of the 128 LMW-AR binding sites identified a total of 118 genes that were closest to the AR binding site (Table 1). Only 20% of the LMW-AR chromosomal binding sites were located within 2Kb up- or down-stream from the transcription start sites (Table 1). Notably, about 20% of the binding sites were more than 10kb up-stream of the transcriptional start site and 9% of the sites were more than 10kb down-stream of the transcriptional end site. This result is consistent with other reports that in LNCaP cells the majority of the AR binding sites are far away from the androgen-regulated genes [25, 26]. Interestingly, several genes (CGI-115, EPHX1, RGPD5, LPP, RHOH, MAT2B, CYP3A43, ANKRD20A3, TMEM60 and GOLGA8G) had two sites bound by the LMW-AR, and in all of the cases except (RGPD5) the two binding sites in each gene were within close vicinity (35 up to 4551bp apart).

***The expression profiles of genes adjacent to LMW-AR binding sites***

To correlate AR binding to gene expression we examined the gene expression profiles of Rv1 cells proliferating in androgen-depleted media and cell stimulated for 2 hours with 10 nM of DHT, conditions that were identical to conditions used to the ChIP-on-chip studies. The Affymatix HG-U133 Plus2.0 Gene Chip microarray analysis was conducted in duplicates. We chose the two hour time point to identify transcripts that are most likely to be direct AR targets. Analysis of the microarray data identified a total of 688 genes differentially expressed (fold change ≥1.5; $P \leq 0.05$) in Rv1 cells in response to DHT in 2hr. Of the 118 closest genes identified in the ChIP-on-chip study of AR binding in the absence of androgen, we found 6 genes (CDKN1B/p27, FABP7, IL-6R, KRIT1, SMA4 and UGT2B15) showed differential

expression in response to DHT (Figure 7A). It has been reported that CDKN1B/p27 and UGT2B15 are androgen-responsive genes [36, 37]. Interestingly, a significant enrichment of AR binding sites was observed at CDKN1B/p27 gene locus, which corresponded with the up-regulation of its expression 2hr post DHT addition. When the analysis included the neighbor genes near the 128 sites, 13 (13/128=10%) were differentially regulated by androgen. Some of the genes were over 50,000 bp from the AR binding site. When the criteria for identifying androgen-regulated genes were relaxed (fold change ≥1.3; P ≤ 0.10), 56 (56/128=44%) of the sites were associated with genes that were androgen regulated. This suggests that for some genes LMW-AR binding in the absence of androgens is not functional or not sufficient and FL-AR is required for their maximal gene regulation.

To further investigate the role of LMW-AR in gene regulation, the expression of several closest genes was analyzed in the absence of androgen following treatment with calpeptin for 48hr. Since treatment with calpeptin reduces LMW-AR expression and the amount of LMW-AR present in the nucleus (Figure 7B), this allows us to study the transcriptional regulation of genes adjacent to the potential LMW-AR binding sites. We examined the effect of LMW-AR inhibition on the expression of the above six closest genes (CDKN1B/p27, FABP7, IL-6R, KRIT1, SMA4 and UGT2B15) that showed differential expression after adding DHT for 2hr. Varied responses to the inhibition of LMW-AR were observed (Figure 7A). The expression of UGT2B15 was down-regulated after adding DHT. Interestingly, inhibition of LMW-AR also significantly reduced their expression, indicating that LMW-AR might function as an activator whereas FL-AR functions as a repressor of the gene. The expression of IL-6R, on the other hand, was elevated after adding DHT. Inhibition of LMW-AR also significantly enhanced its expression, indicating that LMW-AR might function as a repressor while the FL-AR an activator of the gene. Addition of DHT strongly up-regulated the expression of FABP7 and SMA4 (Figure 7A). Inhibition of LMW-AR showed slightly reduction on their expression, indicating that LMW-AR acts like FL-AR as an activator of the genes, but much weaker than FL-AR. While modestly up-regulated by FL-AR after adding DHT, no effect was observed on the expression of CDKN1B/p27 and KRIT1 when LMW-AR was inhibited (Figure 7A), indicating that LMW-AR binding might be non-functional.

Since our preliminary studies suggested that at least half of the hinge domain was removed on the LMW-AR (unpublished), we hypothesized that the failure to interact with the hinge region interacting co-regulators contributed to the functional differences between FL-AR and LMW-AR. Filamin A has been reported to repress AR-dependent transcription by interacting with hinge domain [38]. We analyzed the endogenous gene expression of UGT2B15 in DHT for 2hr or in the absence of androgen following siRNA-mediated silencing of filamin A. As shown in Figure 7C, anti-filamin A siRNA reduced its mRNA level to 11%. Silencing of filamin A expression relieved repression of UGT2B15 in the presence of DHT (Figure 7C: ‘siRNA control AD-‘ vs. ‘siRNA control DHT 2hr’ and ‘FLN siRNA DHT 2hr’), indicating that filamin A is the co-repressor of FL-AR in the suppression of the gene. Silencing of filamin A in the absence of androgen, on the other hand, showed no effect on the expression of UGT2B15 (Figure 7C: ‘siRNA control AD-’ vs. ‘FLN siRNA AD-’), indicating that the regulation activity of LMW-AR is not affected by fimalin A. This suggests that the difference in their interaction with co-regulator filamin A contributes to the different transcriptional outcome of FL- and LMW-AR.

**Key Research Accomplishments**

In current study, we showed that:

- Calpain 2 also plays a role in the generation of the LMW-AR in R1 cells.
- Two distinct mechanisms resulting in elevated levels of LMW-AR by proteolysis. Rv1 cells express low levels of calpain 2 and show low calpain protease activity. Nevertheless, the Rv1 AR is highly sensitive to calpain proteolysis *in vitro* and *in vivo* due to its insertion mutation. On the other hand, R1 cells express high levels of calpain 2 and have high levels of the calpain 2 protease activity, resulting in the proteolysis of the AR.
- Ras-Raf-MEK-ERK signaling pathway regulates the levels of the expression of the LMW forms of AR in Rv1 and R1 cells. Inhibition of ERK phosphorylation by a MEK inhibitor reduces ERK phoshorylation and reduces the expression of the LMW forms. Conversely, activating the Ras-Raf-Mek-ERK by TPA activation of protein kinase C (PKC) increases ERK phosphorylation and the expression of the LMW-AR in both cell types.
- 128 previous unknown binding sites by LMW-AR in Rv1 cells in the absence of androgen. Consistent with others finding, only 6% of the binding sites contain canonical ARE motif and only 20% were located within 2Kb up- or down-stream of the transcriptional start site of the adjacent genes.
- A subset of genes adjacent to the LMW-AR binding sites were differentially expressed in response to the stimulation of DHT for 2hr, indicating the requirement of FL-AR for their maximal transcriptional regulation.
- Some genes were transcriptionally regulated by both LMW-AR and FL-AR, but in an different manner.

**Reportable Outcomes**

We have submitted a manuscript (title: Erk Regulates Calpain2 Induced Androgen Receptor Proteolysis in CWR22 Relapsed Prostate Tumor Cell Lines) to JBC.

The author Honglin Chen obtained her Ph.D. degree in June, 2009.

## Conclusions

Androgen ablation therapy is effective in treating androgen-dependent prostate tumors; however, tumors that can proliferate in castrate levels of androgen eventually arise. We previously reported that in CWR22Rv1 (Rv1) cells, the protease calpain 2 can cleave the androgen receptor (AR) into a constitutively active ~80 KDa low molecular weight (LMW) form. In this study, we further dissect the mechanisms that produce the AR LMW forms using Rv1 cells and the related CWR22-R1 (R1) cells. The 39 a.a. insertional mutation in Rv1 cells sensitizes this AR (E3DM-AR) calpain 2 proteolysis. R1 cells encode the same AR molecule as the parental CWR22 xenograft. Using anti-calpain 2 siRNA and calpeptin, we find that calpain 2 plays a role in the generation of the LMW-AR in R1 cells. Furthermore, LMW-AR expression is regulated by the activation of calpain 2 by Extracellular Signal-Regulated Kinases 1/2 (ERK). Inhibition of ERK phosphorylation or siRNA-mediate decrease of ERK expression reduces LMW-AR levels in R1 cells. Conversely, activation of the MAPK pathway and increased ERK phosphorylation results in increased levels of LMW-AR. Finally, analyses of human tumor samples found that LMW-AR levels are higher in tumors that have an increased calpain/calpastatin ratio and/or increased levels of phospho-ERK (pERK), suggesting that a higher calpain/calpastatin ratio collaborates with activation of the MAP kinase pathway to promote the generation of the LMW-AR. Furthermore, cellular localization analysis of AR shows that the LMW-AR is the predominant form (~90%) present in the nucleus in Rv1 cells cultured in the absence of androgen, allowing us to study the chromosomal binding sites of LMW-AR using chromatin immunoprecipitation (ChIP) combined with DNA microarray analysis (ChIP-on-chip). Using a human promoter array, a total of 128 potential LMW-AR chromosomal binding sites are identified in the absence of androgen and they are also present in the presence of androgen. We find that the majority of the binding sites contain no AR-responsive elements (AREs) and are distant (>2kb) from the transcriptional start sites. Corresponding expression array studies identify that only a subset of genes in the vicinity of LMW-AR binding sites respond to the stimulation of dihydrotestosterone (DHT). Moreover, quantitative RT-PCR analysis shows that LMW-AR can transcriptoinally regulate certain genes in a different manner as full-length (FL) AR.

**References**


1. Chen, C.D., et al., *Molecular determinants of resistance to antiandrogen therapy.* Nat Med, 2004. **10**(1): p. 33-9.
2. Gregory, C.W., et al., *A mechanism for androgen receptor-mediated prostate cancer recurrence after androgen deprivation therapy.* Cancer Res, 2001. **61**(11): p. 4315-9.
3. Gregory, C.W., et al., *Androgen receptor up-regulates insulin-like growth factor binding protein-5 (IGFBP-5) expression in a human prostate cancer xenograft.* Endocrinology, 1999. **140**(5): p. 2372-81.
4. Ruizeveld de Winter, J.A., et al., *Androgen receptor expression in human tissues: an immunohistochemical study.* J Histochem Cytochem, 1991. **39**(7): p. 927-36.
5. Xia, L., et al., *Identification of human male germ cell-associated kinase, a kinase transcriptionally activated by androgen in prostate cancer cells.* J Biol Chem, 2002. **277**(38): p. 35422-33.
6. Shang, Y., M. Myers, and M. Brown, *Formation of the androgen receptor transcription complex.* Mol Cell, 2002. **9**(3): p. 601-10.
7. Taplin, M.E. and S.P. Balk, *Androgen receptor: a key molecule in the progression of prostate cancer to hormone independence.* J Cell Biochem, 2004. **91**(3): p. 483-90.
8. Berrevoets, C.A., A. Umar, and A.O. Brinkmann, *Antiandrogens: selective androgen receptor modulators.* Mol Cell Endocrinol, 2002. **198**(1-2): p. 97-103.
9. Louie, M.C., et al., *Androgen-induced recruitment of RNA polymerase II to a nuclear receptor-p160 coactivator complex.* Proc Natl Acad Sci U S A, 2003. **100**(5): p. 2226-30.
10. Visakorpi, T., et al., *In vivo amplification of the androgen receptor gene and progression of human prostate cancer.* Nat Genet, 1995. **9**(4): p. 401-6.
11. Linja, M.J., et al., *Amplification and overexpression of androgen receptor gene in hormone-refractory prostate cancer.* Cancer Res, 2001. **61**(9): p. 3550-5.
12. Marcelli, M., et al., *Androgen receptor mutations in prostate cancer.* Cancer Res, 2000. **60**(4): p. 944-9.
13. Tilley, W.D., et al., *Mutations in the androgen receptor gene are associated with progression of human prostate cancer to androgen independence.* Clin Cancer Res, 1996. **2**(2): p. 277-85.
14. Veldscholte, J., et al., *A mutation in the ligand binding domain of the androgen receptor of human LNCaP cells affects steroid binding characteristics and response to anti-androgens.* Biochem Biophys Res Commun, 1990. **173**(2): p. 534-40.
15. Wilding, G., M. Chen, and E.P. Gelmann, *Aberrant response in vitro of hormone-responsive prostate cancer cells to antiandrogens.* Prostate, 1989. **14**(2): p. 103-15.
16. Zhao, X.Y., et al., *Glucocorticoids can promote androgen-independent growth of prostate cancer cells through a mutated androgen receptor.* Nat Med, 2000. **6**(6): p. 703-6.
17. Tan, J., et al., *Dehydroepiandrosterone activates mutant androgen receptors expressed in the androgen-dependent human prostate cancer xenograft CWR22 and LNCaP cells.* Mol Endocrinol, 1997. **11**(4): p. 450-9.
18. Jenster, G., et al., *Domains of the human androgen receptor involved in steroid binding, transcriptional activation, and subcellular localization.* Mol Endocrinol, 1991. **5**(10): p. 1396-404.

19. Ceraline, J., et al., *Constitutive activation of the androgen receptor by a point mutation in the hinge region: a new mechanism for androgen-independent growth in prostate cancer.* Int J Cancer, 2004. **108**(1): p. 152-7.
20. Pelley, R.P., et al., *Calmodulin-androgen receptor (AR) interaction: calcium-dependent, calpain-mediated breakdown of AR in LNCaP prostate cancer cells.* Cancer Res, 2006. **66**(24): p. 11754-62.
21. Libertini, S.J., et al., *Evidence for calpain-mediated androgen receptor cleavage as a mechanism for androgen independence.* Cancer Res, 2007. **67**(19): p. 9001-5.
22. Yang, H., et al., *Calpain-mediated androgen receptor breakdown in apoptotic prostate cancer cells.* J Cell Physiol, 2008. **217**(3): p. 569-76.
23. Bernstein, B.E., et al., *Genomic maps and comparative analysis of histone modifications in human and mouse.* Cell, 2005. **120**(2): p. 169-81.
24. Cawley, S., et al., *Unbiased mapping of transcription factor binding sites along human chromosomes 21 and 22 points to widespread regulation of noncoding RNAs.* Cell, 2004. **116**(4): p. 499-509.
25. Wang, Q., et al., *A hierarchical network of transcription factors governs androgen receptor-dependent prostate cancer growth.* Mol Cell, 2007. **27**(3): p. 380-92.
26. Takayama, K., et al., *Identification of novel androgen response genes in prostate cancer cells by coupling chromatin immunoprecipitation and genomic microarray analysis.* Oncogene, 2007. **26**(30): p. 4453-63.
27. Carroll, J.S., et al., *Genome-wide analysis of estrogen receptor binding sites.* Nat Genet, 2006. **38**(11): p. 1289-97.
28. Wainstein, M.A., et al., *CWR22: androgen-dependent xenograft model derived from a primary human prostatic carcinoma.* Cancer Res, 1994. **54**(23): p. 6049-52.
29. Tepper, C.G., et al., *Characterization of a novel androgen receptor mutation in a relapsed CWR22 prostate cancer xenograft and cell line.* Cancer Res, 2002. **62**(22): p. 6606-14.
30. Gregory, C.W., et al., *Androgen receptor stabilization in recurrent prostate cancer is associated with hypersensitivity to low androgen.* Cancer Res, 2001. **61**(7): p. 2892-8.
31. Gregory, C.W., B. He, and E.M. Wilson, *The putative androgen receptor-A form results from in vitro proteolysis.* J Mol Endocrinol, 2001. **27**(3): p. 309-19.
32. Libertini, S.J., et al., *Cyclin E both regulates and is regulated by calpain 2, a protease associated with metastatic breast cancer phenotype.* Cancer Res, 2005. **65**(23): p. 10700-8.
33. Zhang, W., R.D. Lane, and R.L. Mellgren, *The major calpain isozymes are long-lived proteins. Design of an antisense strategy for calpain depletion in cultured cells.* J Biol Chem, 1996. **271**(31): p. 18825-30.
34. Glading, A., et al., *Epidermal growth factor receptor activation of calpain is required for fibroblast motility and occurs via an ERK/MAP kinase signaling pathway.* J Biol Chem, 2000. **275**(4): p. 2390-8.
35. Lee, H.W., et al., *Phorbol 12-myristate 13-acetate up-regulates the transcription of MUC2 intestinal mucin via Ras, ERK, and NF-kappa B.* J Biol Chem, 2002. **277**(36): p. 32624-31.
36. Chen, Y., et al., *Expression of G1 cyclins, cyclin-dependent kinases, and cyclin-dependent kinase inhibitors in androgen-induced prostate proliferation in castrated rats.* Cell Growth Differ, 1996. **7**(11): p. 1571-8.

37. Bao, B.Y., et al., *Androgen receptor mediates the expression of UDP-glucuronosyltransferase 2 B15 and B17 genes.* Prostate, 2008. **68**(8): p. 839-48.
38. Loy, C.J., K.S. Sim, and E.L. Yong, *Filamin-A fragment localizes to the nucleus to regulate androgen receptor and coactivator functions.* Proc Natl Acad Sci U S A, 2003. **100**(8): p. 4562-7.

**Supporting Data**

Fig.1. Rv1 and R1 cell proliferate in castrate levels of androgen. A. R1 and Rv1 cells proliferating in the presence of androgen (Ad+) are less refractile than cells in androgen depleted media (Ad-). B. AR expression is greater in R1 than in Rv1 cells, but the FL and LMW AR expressed in R1 cells is slightly smaller that that expressed in Rv1 cells. C. R1 and Rv1 cells proliferate in castrate levels of androgen, but proliferation is slightly greater in the presence of androgen. Androgen depletion inhibits LNCaP proliferation. D. Rv1 and R1 cells proliferate in the presence of 10uM Casodex.

Fig 2. Calpain expression and activity in prostate derived cells. A. Inhibition of calpain activity in R1 cells with calpeptin (60uM) for 48 h decreases the expression of the LMW-AR. B. Top panel: Western blot analysis of calpain 2 expression in non-transformed and tumor prostate cells. Bottom panel: Western blot analysis of calpastatin levels in non-transformed and tumor cells. GAPDH served as a loading control. C. Calpain-dependent proteolysis of FAK from a 120 KDa form to 90 KDa and ultimately smaller forms is indicative of calpain activity. FAK proteolysis is greater in R1 than in Rv1 cells and is greater in both cells in the absence of androgens. D. Calpain 2 siRNA down-regulated calpain 2 protein levels of calpain 2 144 h post transfection in R1 cells. The down-regulation of calpain 2 expression by anti-calpain 2 siRNA reduced the LMW-AR and calpain-dependent proteolysis of FAK. E. Expression of CLDN4 in R1 cells culture in androgen depleted media, following a 2 h stimulation with DHT and a 24 h treatment with 60uM calpeptin was assessed by real time PCR. CLDN4 expression was standardized to GAPDH.

Fig 3. Transient expression of wt and E3DM-AR cDNA in PC3 cells. A. Transfection of PC3 cells with wt or E3DM-AR cDNA results in the expression of FL and LMW (denoted by arrows and brackets) forms of AR. The 3 nonspecific (NS) bands at ~ 80 KDa present in the non-transfected PC3 cells serve as markers (denoted by dots). The FL and LMW forms expressed in cells transfected with the E3DM-AR are slightly larger. B. Extracts prepared from PC3 cells transfected with wt or E3DM-AR were treated with 1M $CaCl_2$ to activate calpain activity. The E3DM-AR is degraded more rapidly than the WT AR. (Compare lane 1 and 6; 2 and 7; 4 and 9).

Fig 4. Inhibition of ERK phosphorylation reduces the expression of the LMW-AR. A. Western blot analysis of ERK expression in non-transformed and tumor-derived cells lines. B. The pERK levels are higher in R1 than Rv1 cells in the presence or absence of androgen. C. R1 cells were treated with 20 uM of the MEK inhibitor U0126 (I) or vehicle (C) for 24 or 48 hours in the presence or absence of androgens. The top portion of the blot shown in top panel was used to detect the expression of AR. Inhibition of ERK phosphorylation reduced the expression of the LMW-AR. The arrows denote the FL and ~ 80 KDa LMW-AR. D. ERK specific siRNA reduced the expression of pERK and the levels of LMW AR.

Fig 5. ERK activation and calpain/calpastatin ratios collaborate to promote expression of the LMW AR. A. Treatment of R1 and Rv1 cells with TPA (10 nM) for 1 and 2 hours increases the expression of the LMW-AR forms (top panel). Control cells were treated with DMSO. The bottom panel shows that TPA treatment increases pERK levels. B. Higher calpain/calpastatin and pERK levels together correlate with higher expression of LMW AR in tumor samples. C. Quantitation of the expression data in panel B. The calpain/calpastatin rations multiplied by levels of pERK are significantly higher in samples with elevated levels of LMW-AR.

Figure 6. The identification of the potential chromosomal binding sites of LMW AR in Rv1 cells by ChIP-on-chip assay. A. The cytoplasmic and nuclear extracts showed the cellular location of the FL- and LMW-AR in Rv1 and R1 cells in the absence and presence of androgen. B. The diagram showed the number of the overlapping chromosomal binding sites identified in Rv1 cells cultured in the absence of androgen (orange) or stimulated with DHT for 2hr (yellow) and in R1 cells stimulated with DHT for 2hr (yellow). C. An extensive view of the binding sites in chromosome 12 identified in Rv1 cells cultured in the absence of androgen (Rv1-AD-) or stimulated by DHT for 2hr (Rv1_AD+) (top panel). A closer view of the binding sites around the gene CDKN1B in Rv1 cells cultured in the absence androgen or stimulated by DHT for 2hr (bottom panel). The graph was generated using UCSC genome browser. D. A pie chart showing the distribution of the binding motifs of AR in the absence of androgen (AD-) or in response to DHT for 2hr.

Figure 7. Transcriptional regulation of LMW-AR in Rv1 cells. (A). Real-time PCR analysis of LMW-AR bound genes in response to DHT stimulation or inhibition of LMW-AR expression by calpeptin treatment. Rv1 cells proliferated in the absence of androgen were incubated with10nM DHT for 2hr or 40uM calpeptin for 48hr. (B). Calpeptin treatment reduced the amount of LMW-AR in the Rv1 nucleus extract. Rv1 cells proliferated in the absence of androgen were treated with 40uM calpeptin for 48hr. Cells were harvested, fractionated and subject to Western blot. The band is the LMW-AR and FL-AR is invisible on this blot. (C). Real-time PCR analysis of Filamin A and UGT2B15. Rv1 cells proliferated in the absence of androgen were treated with anti-filamin A siRNA or control siRNA for 72hr, then harvested for RNA extraction, or treated with 10nM DHT for 2hr and then harvested for RNA extraction.

Figure 1

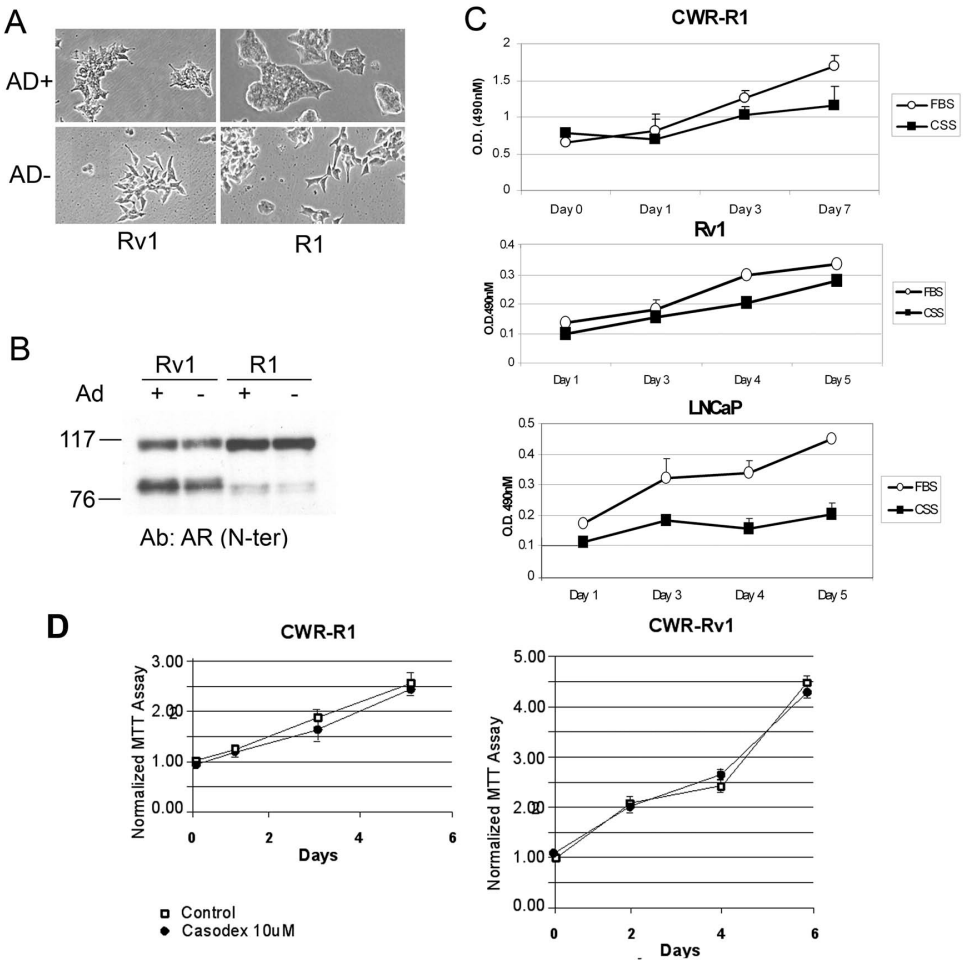
A
AD+
AD-
Rv1
R1
B
Rv1
R1
Ad
+
-
+
-
117
76
Ab: AR (N-ter)
C
CWR-R1
O.D. (490nM)
FBS
CSS
Day 0
Day 1
Day 3
Day 7
Rv1
O.D.490nM
Day 1
Day 3
Day 4
Day 5
LNCaP
D
CWR-R1
Normalized MTT Assay
Days
Control
Casodex 10uM
CWR-Rv1

Figure 2

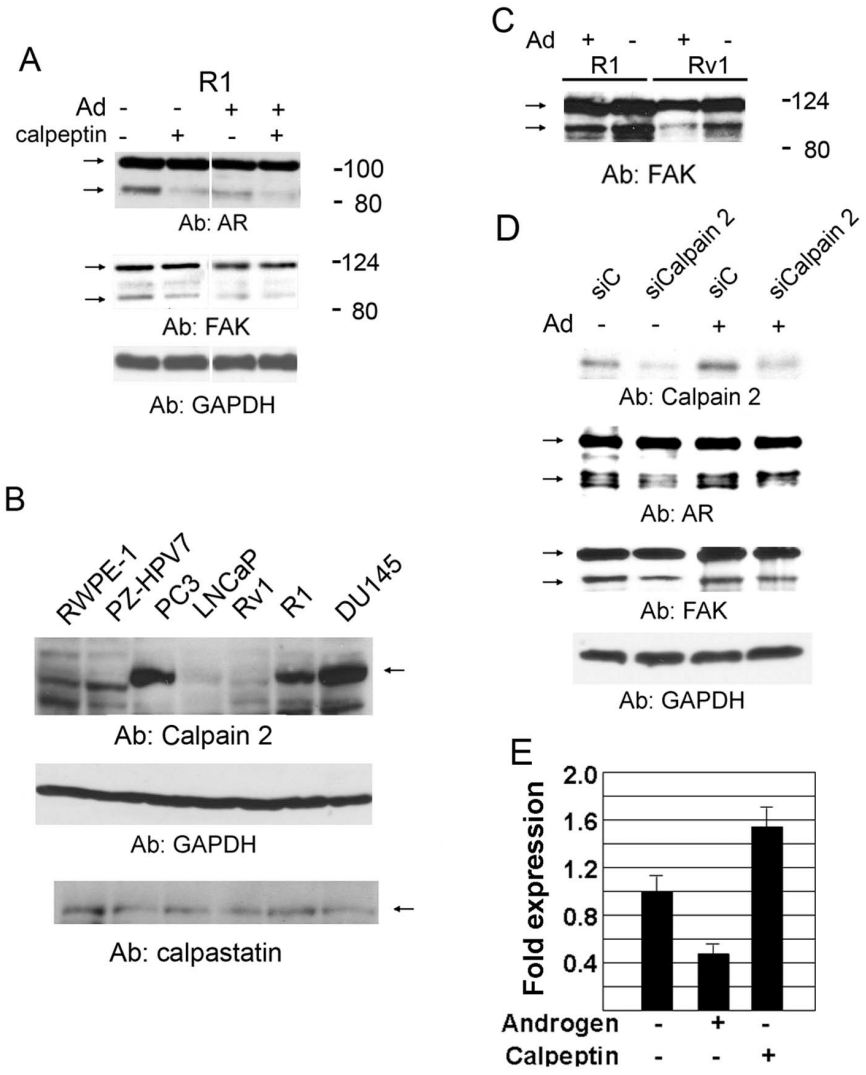
A
R1
Ad - - + +
calpeptin - + - +
-100
- 80
Ab: AR
-124
- 80
Ab: FAK
Ab: GAPDH
B
RWPE-1
PZ-HPV7
PC3
LNCaP
Rv1
R1
DU145
Ab: Calpain 2
Ab: GAPDH
Ab: calpastatin
C
Ad + - + -
R1
Rv1
-124
- 80
Ab: FAK
D
siC
siCalpain 2
siC
siCalpain 2
Ad - - + +
Ab: Calpain 2
Ab: AR
Ab: FAK
Ab: GAPDH
E
Fold expression
2.0
1.6
1.2
0.8
0.4
Androgen - + -
Calpeptin - - +

Figure 3

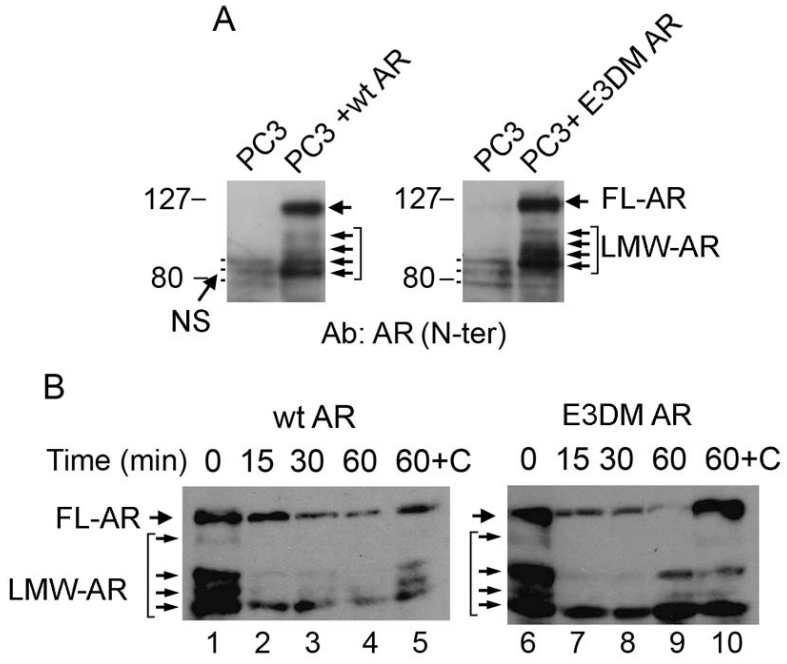
A
PC3
PC3 +wt AR
PC3
PC3+ E3DM AR
127–
80 –
NS
127–
80 –
FL-AR
LMW-AR
Ab: AR (N-ter)
B
wt AR
E3DM AR
Time (min) 0 15 30 60 60+C
0 15 30 60 60+C
FL-AR
LMW-AR
1 2 3 4 5
6 7 8 9 10

Figure 4

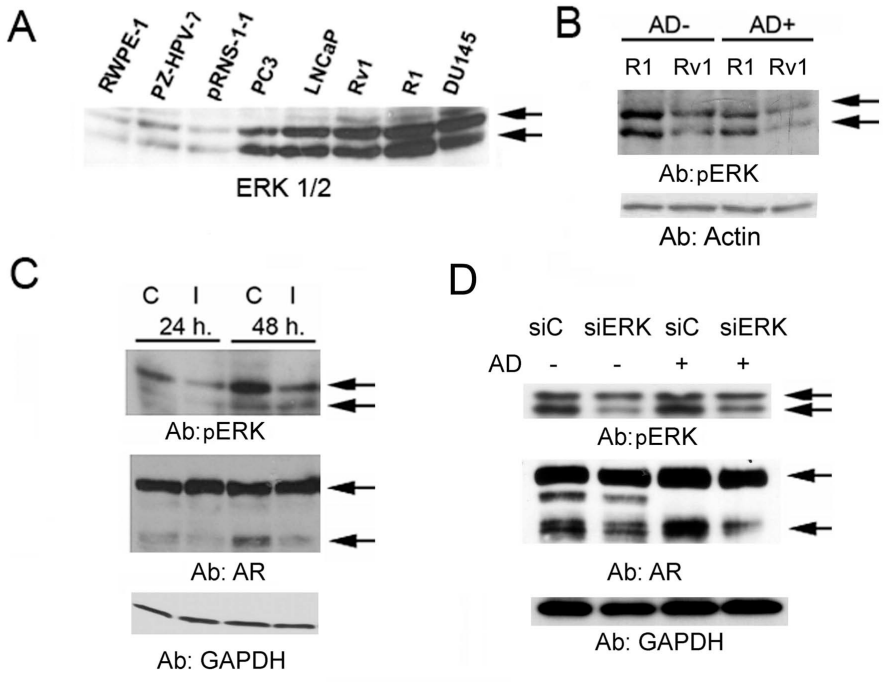
A
RWPE-1
PZ-HPV-7
pRNS-1-1
PC3
LNCaP
Rv1
R1
DU145
ERK 1/2
B
AD-
AD+
R1
Rv1
R1
Rv1
Ab:pERK
Ab: Actin
C
C
I
C
I
24 h.
48 h.
Ab:pERK
Ab: AR
Ab: GAPDH
D
siC
siERK
siC
siERK
AD
-
-
+
+
Ab:pERK
Ab: AR
Ab: GAPDH

Figure 5

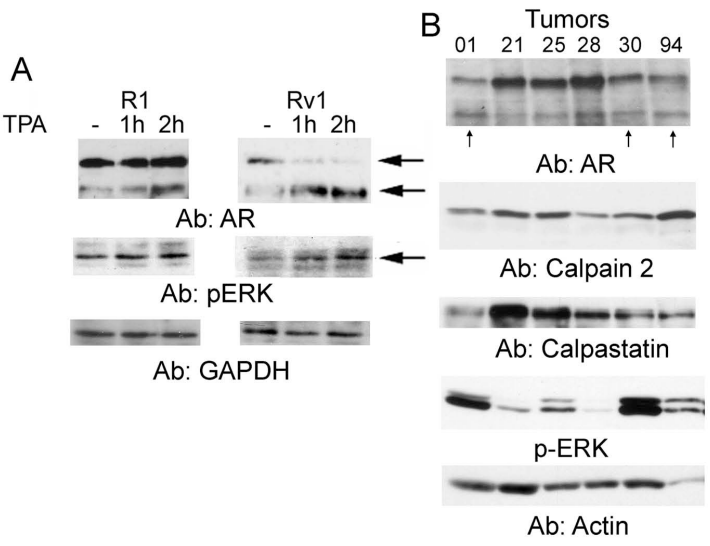





C

| Sample | 01 | 21 | 25 | 28 | 30 | 94 |
|---|---|---|---|---|---|---|
| pERK | 1.29 | 0.28 | 0.79 | 0.22 | 1.93 | 2.15 |
| Calpastatin | 0.90 | 1.70 | 2.02 | 1.36 | 0.93 | 2.01 |
| Calpain | 0.75 | 0.76 | 1.13 | 0.66 | 0.81 | 3.06 |
| pERK x $\frac{\text{Calpain}}{\text{Calpastatin}}$ | 1.07 | 0.12 | 0.44 | 0.11 | 1.68 | 3.27 |

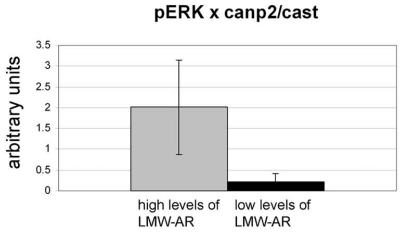

Figure 6

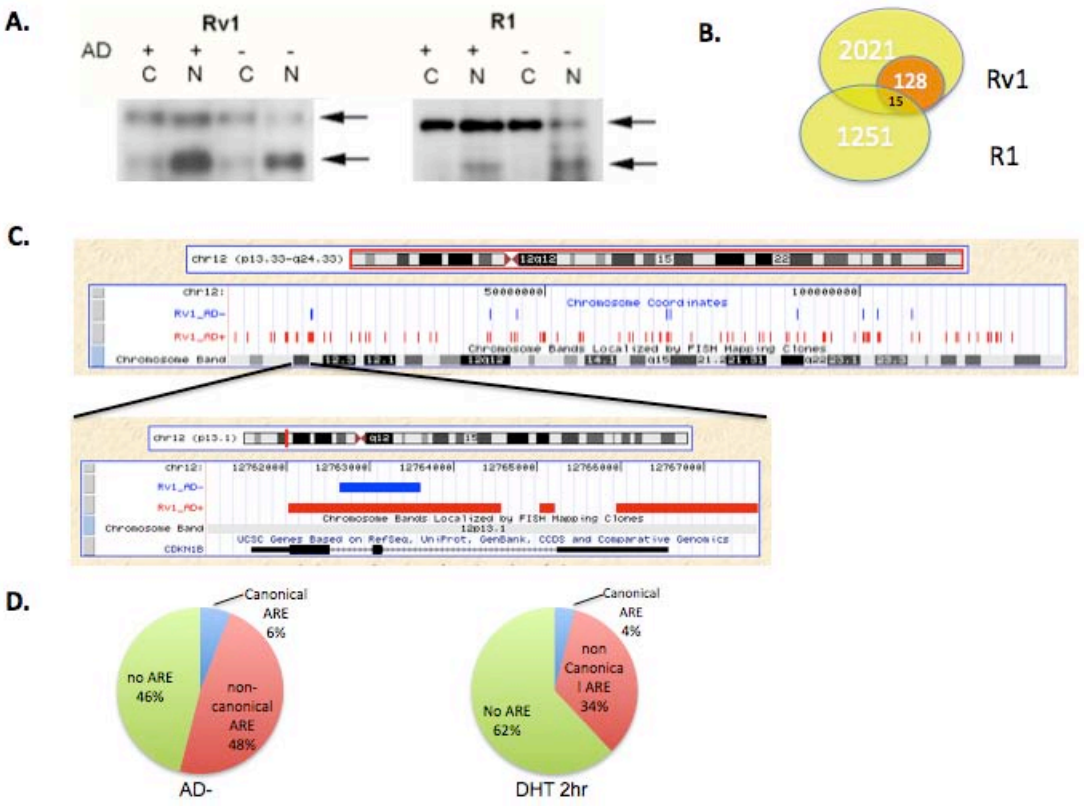
A.
Rv1
R1
AD
+ + - -
C N C N
B.
2021
128
15
1251
Rv1
R1
C.
chr12 (p13.33-q24.33)
Chromosome Coordinates
Rv1_AD-
Rv1_AD+
Chromosome Bands Localized by FISH Mapping Clones
Chromosome Band
chr12 (p13.1)
UCSC Genes Based on RefSeq, UniProt, GenBank, CCDS and Comparative Genomics
CDKN1B
D.
Canonical ARE 6%
no ARE 46%
non-canonical ARE 48%
AD-
Canonical ARE 4%
non Canonical ARE 34%
No ARE 62%
DHT 2hr

Figure 7

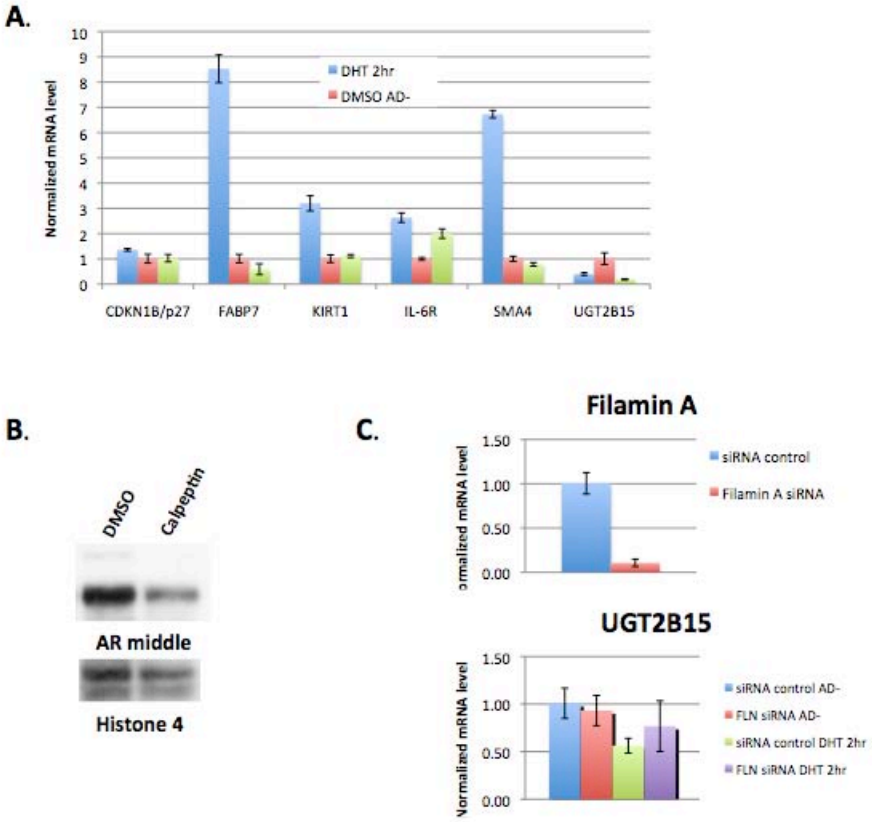
A.
Normalized mRNA level
DHT 2hr
DMSO AD-
CDKN1B/p27
FABP7
KIRT1
IL-6R
SMA4
UGT2B15
B.
DMSO
Calpeptin
AR middle
Histone 4
C.
Filamin A
siRNA control
Filamin A siRNA
UGT2B15
siRNA control AD-
FLN siRNA AD-
siRNA control DHT 2hr
FLN siRNA DHT 2hr

**Table 1. The list of potential LMW-AR chromosomal binding sites identified by ChIP-on-chip in Rv1 cells cultured in androgen depleted medium.**

| chromosome | | start | end | FDR | Closest gene | distance_to_TSS | location |
|---|---|---|---|---|---|---|---|
| chr1 | | 16864805 | 16865837 | 0.05 | NBPF1 | -52753 | TSS_upstream |
| | | 22136758 | 22137152 | 0.00 | HSPG2 | -622 | TSS_upstream |
| | * | 42578210 | 42578867 | 0.05 | FOXJ3 | -5049 | TSS_upstream |
| | | 85111676 | 85111897 | 0.05 | EDG7 | -7357 | TSS_upstream |
| | | 152657272 | 152657555 | 0.04 | IL6R | 13121 | intron |
| | * | 159635314 | 159635709 | 0.05 | C1orf192 | -31224 | TSS_upstream |
| | | 161110301 | 161110770 | 0.05 | C1orf110 | -5307 | TSS_upstream |
| | | 205563333 | 205563694 | 0.00 | CD55 | 234307 | TES_downstream |
| | | 208025311 | 208026089 | 0.04 | C1orf74 | -1188 | TSS_upstream |
| | | 216522748 | 216523246 | 0.00 | CGI-115 | -2277 | TSS_upstream |
| | | 216524107 | 216524509 | 0.05 | CGI-115 | -966 | TSS_upstream |
| | | 224074724 | 224075447 | 0.02 | EPHX1 | -4513 | TSS_upstream |
| | | 224076182 | 224076536 | 0.03 | EPHX1 | -3239 | TSS_upstream |
| | | 226930302 | 226930964 | 0.05 | RHOU | -6858 | TSS_upstream |
| | | 227474815 | 227475660 | 0.05 | RAB4A | 1736 | intron |
| | | 227687485 | 227687790 | 0.05 | NUP133 | 23073 | intron |
| chr2 | | 9068246 | 9068784 | 0.05 | MBOAT2 | -7189 | TSS_upstream |
| | * | 61096462 | 61097660 | 0.00 | FLJ32312 | 1650 | 5'UTR |
| | | 96709406 | 96710018 | 0.02 | LOC90342 | -15208 | TSS_upstream |
| | | 102100298 | 102100788 | 0.05 | IL1R1 | -36290 | TSS_upstream |
| | | 109906570 | 109906985 | 0.02 | RGPD7 | -846 | TSS_upstream |
| | | 110771915 | 110772458 | 0.02 | RGPD5 | -282326 | TSS_upstream |
| | | 111053390 | 111053866 | 0.05 | RGPD5 | -851 | TSS_upstream |
| | * | 121756809 | 121757420 | 0.05 | TFCP2L1 | 2130 | intron |
| | | 135313183 | 135314419 | 0.00 | ACMSD | 1146 | intron |
| | | 217188354 | 217189045 | 0.05 | IGFBP2 | -17672 | TSS_upstream |
| | | 238433717 | 238434904 | 0.00 | RAMP1 | 1385 | intron |
| | | 241681282 | 241681890 | 0.02 | MTERFD2 | 8810 | 3'UTR |
| chr3 | | 95228036 | 95228573 | 0.05 | STX19 | 1839 | 5'UTR |
| | | 155525085 | 155526261 | 0.00 | DHX36 | -709 | TSS_upstream |
| | | 170972672 | 170973372 | 0.00 | MYNN | -524 | TSS_upstream |
| | | 184090480 | 184091149 | 0.00 | ATP11B | 96830 | intron |
| | | 189407063 | 189407672 | 0.00 | LPP | -6047 | TSS_upstream |
| | | 189411186 | 189411946 | 0.00 | LPP | -1848 | TSS_upstream |
| chr4 | | 39868356 | 39869125 | 0.02 | RHOH | -6256 | TSS_upstream |
| | | 39869633 | 39869883 | 0.05 | RHOH | -5238 | TSS_upstream |
| | | 57242033 | 57242991 | 0.05 | HOP | -191 | TSS_upstream |
| | * | 69116609 | 69117122 | 0.05 | UGT2B17 | -26 | TSS_upstream |
| | * | 69570641 | 69571326 | 0.02 | UGT2B15 | -5 | TSS_upstream |
| | | 71417985 | 71418195 | 0.05 | UNQ689 | -796 | TSS_upstream |

| | | | | | | | |
|---|---|---|---|---|---|---|---|
| | | 83631386 | 83632082 | 0.02 | MASA | 60948 | TES_downstream |
| | | 104160587 | 104161189 | 0.00 | LOC150159 | -564 | TSS_upstream |
| | | 116253672 | 116254863 | 0.05 | NDST4 | 213 | 5'UTR |
| chr5 | | 17358364 | 17359521 | 0.00 | BASP1 | 88193 | TES_downstream |
| | | 43075976 | 43077397 | 0.05 | LOC389289 | -589 | TSS_upstream |
| | | 69043534 | 69043826 | 0.05 | SMA4 | -32839 | TSS_upstream |
| | | 69174442 | 69174858 | 0.05 | GUSBP1 | -60708 | TSS_upstream |
| | | 71046170 | 71046891 | 0.00 | CARTPT | -4219 | TSS_upstream |
| | | 95003096 | 95003955 | 0.00 | RFESD | -4816 | TSS_upstream |
| | | 132412520 | 132413483 | 0.00 | HSPA4 | -2559 | TSS_upstream |
| | | 133356892 | 133357581 | 0.05 | VDAC1 | 11095 | 5'UTR |
| | * | 147271350 | 147271821 | 0.05 | MGC23985 | -5328 | TSS_upstream |
| | | 165140913 | 165141810 | 0.05 | MAT2B | 2278553 | TES_downstream |
| | | 165145723 | 165146101 | 0.00 | MAT2B | 2283104 | TES_downstream |
| | | 177409706 | 177410694 | 0.00 | PROP1 | -54352 | TSS_upstream |
| chr6 | | 27555314 | 27555674 | 0.02 | ZNF184 | -6637 | TSS_upstream |
| | | 32481685 | 32482038 | 0.05 | BTNL2 | 1016 | intron |
| | | 35802763 | 35803273 | 0.02 | C6orf81 | -9818 | TSS_upstream |
| | | 123134867 | 123135269 | 0.05 | FABP7 | -7276 | TSS_upstream |
| chr7 | | 77258666 | 77258951 | 0.00 | TMEM60 | 6874 | TES_downstream |
| | | 77259297 | 77259870 | 0.00 | TMEM60 | 6099 | TES_downstream |
| | | 86810485 | 86812436 | 0.05 | CROT | -1486 | TSS_upstream |
| | | 90173344 | 90174014 | 0.05 | PFTK1 | -2968 | TSS_upstream |
| | | 91720528 | 91720823 | 0.02 | KRIT1 | -7512 | TSS_upstream |
| | | 94789986 | 94790898 | 0.05 | PON1 | 1337 | intron |
| | | 99262534 | 99262861 | 0.02 | CYP3A43 | -874 | TSS_upstream |
| | | 99263324 | 99263899 | 0.00 | CYP3A43 | 40 | 5'UTR |
| chr8 | | 1908276 | 1908755 | 0.04 | KBTBD11 | -935 | TSS_upstream |
| | | 1985866 | 1986424 | 0.05 | MYOM2 | 5491 | 5'UTR |
| | | 32618295 | 32618812 | 0.02 | NRG1 | 93259 | intron |
| | * | 62764856 | 62765634 | 0.02 | ASPH | -327 | TSS_upstream |
| | | 81155377 | 81156130 | 0.05 | TPD52 | -189 | TSS_upstream |
| | | 92016257 | 92016819 | 0.02 | EFCBP1 | 143585 | intron |
| | | 95635315 | 95635625 | 0.05 | KIAA1429 | -607 | TSS_upstream |
| | | 104842195 | 104842405 | 0.02 | RIMS2 | -58375 | TSS_upstream |
| | | 134408137 | 134408683 | 0.05 | NDRG1 | -29731 | TSS_upstream |
| chr9 | | 458522 | 459780 | 0.00 | DOCK8 | 196104 | TES_downstream |
| | | 42014216 | 42015102 | 0.00 | MGC218881 | -69629 | TSS_upstream |
| | | 42473311 | 42473672 | 0.05 | ANKRD20A3 | 115193 | TES_downstream |
| | | 43008156 | 43008569 | 0.05 | ANKRD20 | 650064 | TES_downstrea |

| | | | | | | |
|---|---|---|---|---|---|---|
| | | | | A3 | | m |
| | 83490582 | 83491814 | 0.05 | TLE1 | 2217 | intron |
| * | 127099076 | 127099337 | 0.05 | GAPVD1 | 35275 | 5'UTR |
| | 130683610 | 130683946 | 0.05 | CCBL1 | 396 | 5'UTR |
| chr10 | 75005198 | 75007594 | 0.00 | USP54 | -23293 | TSS_upstream |
| | 88842056 | 88843108 | 0.04 | GLUD1 | 2020 | intron |
| | 111752538 | 111753211 | 0.05 | ADD3 | -2841 | TSS_upstream |
| | 114110373 | 114110898 | 0.02 | ACSL5 | -13270 | TSS_upstream |
| chr11 | 76424867 | 76425442 | 0.04 | B3GNT6 | 2047 | 5'UTR |
| | 101688751 | 101689123 | 0.05 | BIRC3 | -4466 | TSS_upstream |
| | 110679133 | 110682583 | 0.00 | FLJ45803 | -5110 | TSS_upstream |
| | 116515530 | 116515766 | 0.00 | PAFAH1B2 | -4601 | TSS_upstream |
| chr12 | 12762638 | 12763601 | 0.05 | CDKN1B | 1544 | exon |
| | 12921346 | 12922113 | 0.05 | GPRC5A | -13493 | TSS_upstream |
| | 41273916 | 41274369 | 0.05 | PRICKLE1 | -4398 | TSS_upstream |
| | 45472464 | 45473769 | 0.00 | SLC38A4 | 32885 | exon |
| | 69324316 | 69324768 | 0.02 | PTPRR | 110089 | intron |
| * | 69842894 | 69844074 | 0.02 | TSPAN8 | 452 | intron |
| | 89919368 | 89919774 | 0.05 | DSPG3 | 3362 | intron |
| * | 100393303 | 100394366 | 0.00 | SPIC | -953 | TSS_upstream |
| | 102787842 | 102789518 | 0.00 | NT5DC3 | -29576 | TSS_upstream |
| | 108233254 | 108234362 | 0.00 | FOXN4 | -2401 | TSS_upstream |
| chr13 * | 27089576 | 27090358 | 0.00 | LNX2 | 2571 | 5'UTR |
| | 31417733 | 31418816 | 0.02 | FRY | -85162 | TSS_upstream |
| | 48871900 | 48872719 | 0.05 | CAB39L | 1190 | 5'UTR |
| chr14 | 52082233 | 52082434 | 0.05 | KIAA1344 | 6629 | 5'UTR |
| | 57128860 | 57129691 | 0.05 | C14orf105 | 323896 | TES_downstream |
| | 67066319 | 67067360 | 0.00 | PLEKHH1 | -2921 | TSS_upstream |
| | 77235294 | 77235817 | 0.02 | ALKBH1 | 8553 | intron |
| chr15 | 20286282 | 20286797 | 0.04 | TUBGCP5 | -98403 | TSS_upstream |
| | 21131612 | 21131948 | 0.00 | FLJ36144 | 111702 | TES_downstream |
| | 26277642 | 26277943 | 0.05 | GOLGA8G | -19612 | TSS_upstream |
| | 26596571 | 26596904 | 0.05 | GOLGA8G | -19580 | TSS_upstream |
| | 40350094 | 40350898 | 0.02 | TMEM87A | 2426 | intron |
| * | 66901192 | 66901763 | 0.02 | ANP32A | -1201 | TSS_upstream |
| * | 89205500 | 89205991 | 0.00 | FURIN | -7143 | TSS_upstream |
| chr16 | 53518414 | 53519450 | 0.02 | IRX5 | -3679 | TSS_upstream |
| chr17 * | 7998727 | 7999908 | 0.00 | PER1 | -2891 | TSS_upstream |
| | 19486254 | 19486717 | 0.05 | ALDH3A2 | -6170 | TSS_upstream |
| chr18 | 19518446 | 19519169 | 0.00 | LAMA3 | -4752 | TSS_upstream |
| | 46811264 | 46812019 | 0.02 | SMAD4 | 1031 | 5'UTR |
| chr20 | 31242786 | 31243701 | 0.00 | C20orf70 | 23623 | TES_downstream |

| | | | | | | |
|---|---|---|---|---|---|---|
| | 57966260 | 57966718 | 0.05 | CDH26 | -387 | TSS_upstream |
| chr22 | 14653344 | 14654277 | 0.00 | ACTBL1 | 14126 | 3'UTR |
| | 19829248 | 19829710 | 0.05 | FLJ42953 | 42175 | TES_downstream |
| | 19949347 | 19950008 | 0.05 | GGT2 | -39096 | TSS_upstream |
| | 43964814 | 43965717 | 0.00 | C22orf9 | 21745 | TES_downstream |
| chrX | 106756502 | 106757108 | 0.02 | PRPS1 | -1609 | TSS_upstream |
| | 128623040 | 128623977 | 0.00 | APLN | -6914 | TSS_upstream |